Article

JOURNAL OF THE CHINESE CHEMICAL SOCIETY

Chemical Composition and Reaction Mechanisms for Aged *p*-Xylene Secondary Organic Aerosol in the Presence of Ammonia

Jun Xu,[a] Ming-Qiang Huang,[a,b] Shun-You Cai,[a] Ying-Min Liao,[b] Chang-Jin Hu,[c] Wei-Xiong Zhao,[c] Xue-Jun Gu[c] and Wei-Jun Zhang[c]

[a]*Fujian Provincial Key Laboratory of Modern Analytical Science and Separation Technology, College of Chemistry & Environment, Minnan Normal University, Zhangzhou 363000, P. R. China*
[b]*College of Environmental Science and Engineering, Xiamen University, Tan Kah Kee College, Zhangzhou 363105, P. R. China*
[c]*Laboratory of Atmospheric Physico-Chemistry, Anhui Institute of Optics and Fine Mechanics, Chinese Academy of Sciences, Hefei 230031, P. R. China*

(Received: July 14, 2017; Accepted: December 11, 2017; Published Online: January 5, 2018; DOI: 10.1002/jccs.201700249)

A laboratory study was carried out to investigate the chemical composition of aged aromatic secondary organic aerosol (SOA) formed from the photoxidation of *p*-xylene in the presence of ammonia (NH_3). The experiments were conducted by irradiating *p*-xylene/CH_3ONO/NH_3 air mixtures without and with NO in a home-made smog chamber. The particulate products of aged *p*-xylene SOA in the presence of NH_3 were measured by UV–vis spectrophotometry, attenuated total reflectance Fourier transform infrared (ATR-FTIR) spectroscopy, and aerosol laser time-of-flight mass spectrometry (ALTOFMS) coupled with the fuzzy C-means (FCM) clustering algorithm. The experimental results show that NH_3 does not alter the gas–particle partitioning in the photoxidation of *p*-xylene without NO and that 2,5-dimethylphenol is the predominant NH_3-aged *p*-xylene SOA without NO. However, NH_3 has a significant promotional effect on the formation of organonitrogen compounds in the OH-initiated oxidation of *p*-xylene with NO. Organic ammonium salts such as ammonium glyoxylate and *p*-methyl ammonium benzoate, which are formed from NH_3 reactions with gaseous organic acids, were detected as the major particulate organonitrogen products of NH_3-aged *p*-xylene SOA with NO. 1*H*-Imidazole, 4-methyl-1*H*-imidazole, and other imidazole products of the heterogeneous reactions between NH_3 and dialdehydes of *p*-xylene SOA were newly measured. The possible reaction mechanisms leading to these organonitrogen products are also discussed and proposed. The formation of imidazole products suggests that some ambient particles containing organonitrogen compounds may be the result of this mechanism. The results of this study may provide valuable information for discussing anthropogenic SOA aging mechanisms.

Keywords: *p*-Xylene; Secondary organic aerosol; Ammonia; Organonitrogen compounds; Aging mechanisms.

INTRODUCTION

p-Xylene and other monocyclic aromatic hydrocarbons emitted from motor vehicles are the main volatile organic compounds (VOCs) in the urban atmosphere.[1,2] After being released into the atmosphere, *p*-xylene can be easily attacked by OH radicals, generating nonvolatile and semivolatile organic compounds, which can result in secondary organic aerosol (SOA) formation via either a self-nucleation process or gas/particle partitioning on pre-existing particulate matter.[1–3] SOA in the atmosphere can have a lifetime of about 1 week,[4,5] during which they can age via the reaction with ammonia (NH_3), nitrogen oxides (NO_x), and other reduced nitrogen substances, leading to the formation of organonitrogen compounds of brown carbon,[6–8] which absorb radiation efficiently in the near-UV (300–400 nm) and short wavelengths of the

*Corresponding author. Email: huangmingqiang@gmail.com

visible range,[9] and are an important contributor to radiative forcing.[9–11]

Ammonia (NH_3) from livestock waste, fertilizers, gasoline vehicles, and other non-agricultural sources is the primary alkaline polluting gas commonly found in the atmosphere.[12,13] Field measurement have shown the background level concentration of NH_3 is less than 500 ppt in remote areas whereas it reaches a few ppm in the urban ammosphere.[14,15] Previous studies have shown that NH_3 plays an important role in the aging of SOA particles. SOA particles formed from the OH- and O_3-initiated oxidation of anthropogenic and biogenic precursors and exposed to NH_3 were studied by Updyke *et al.*,[6] who measured the highest mass absorption coefficients (MACs) of SOA from limonene and sesquiterpenes ozonolysis and matched them with the MAC values of biomass burning particles. The complex refractive indices (RIs) of brown carbon from biogenic SOA aged with NH_3 were measured by Flores *et al.*[7] with broadband cavity-enhanced spectroscopy. The obtained real component (n) of the NH_3-aged biogenic SOA did not change significantly, but the imaginary part (k) increased from $k = 0.000$ to $k = 0.030$ for the NH_3-aged limonene and α-humulene SOA. Also, the formation of particulate nitrogen-containing organic products during the photoxidation of *m*-xylene and ozonolysis of α-pinene with NH_3 were studied by Liu *et al.*[8] A number of organonitrogen fragments were observed, which were in accordance with the reactions between NH_3 and the carbonyl constituents of SOA.

The above experiments mainly focused on the measurement of the optical parameters (MAC, RI) of the NH_3-aged biogenic SOA. However, the chemical constituents of organonitrogen products of brown carbon were not considered in detail in these reports. Our group has used aerosol laser time-of-flight mass spectrometry (ALTOFMS) to measure the *p*-xylene SOA particles in real time and detected aromatic aldehydes, unsaturated dicarbonys, hydroxyl dicarbonys, organic acids, and oligomers.[16] Recently, a fuzzy C-means (FCM) algorithm was developed by our group to classify the mass spectra of a large number of particles. Previous studies had shown that the real-time ALTOFMS detection approach coupled with the FCM algorithm data processing could successfully carry out the cluster analysis of aromatic SOA.[17,18] On this basis, the chemical constituents of particulate products of aged *p*-xylene SOA in the presence of NH_3 without and with NO were measured with UV–vis spectrophotometry, attenuated total reflectance-Fourier transform infrared (ATR-FTIR) spectroscopy, and ALTOFMS coupled with the FCM algorithm. The reaction mechanisms leading to the organonitrogen products of brown carbon are also proposed and discussed in this paper.

EXPERIMENTAL

Smog chamber experiment of *p*-xylene SOA aging

The formation and aging of *p*-xylene SOA were carried out in an 850-L smog chamber equipped with black lamps, similar to the procedure described previously.[16–18] It is worth pointing out that NO emitted from vehicle emissions is the major nitrogen oxide pollutant in the urban atmosphere.[19] It can participate in the photochemical processes of VOCs, leading to the formation of ozone and SOA.[20,21] The rapid development of China's economy and the increasing number of vehicles result in an urban atmosphere containing high concentrations of NO_x.[22] In order to simulate the atmosphere of a Chinese city, NO was added in the current study. After flushing the smog chamber, *p*-xylene, NO, CH_3ONO, and NH_3 were introduced into the chamber, which was then filled with purified air to the full volume. The concentration of *p*-xylene and CH_3ONO was fixed as 2.0 and 20.0 ppm, respectively. The effects of NH_3 on the particulate products of aged *p*-xylene SOA without NO and with 2.0 ppm NO were investigated. In each case, seven experiments were designed with NH_3 absent or present in the concentration of 2, 4, 8, 12, 16, and 20 ppm, respectively. In all experiments, the relative humidity and temperature in the chamber were maintained at about $25 \pm 2\%$ and 300 ± 2 K, respectively. The OH radicals were formed from the irradiation of CH_3ONO using four black lamps.[23] Each experiment was repeated three times in parallel, twice for collecting the aged particles for offline analysis with UV–vis and ATR-FTIR spectrometry after 8 h of photoxidation, and once for online analysis with ALTOFMS coupled with the FCM clustering algorithm.

Chemical characterization with UV–vis and ATR-FTIR

After 8 h of photoxidation, the aged *p*-xylene SOA particles were collected on polytetrafluoroethylene membrane filters (Sigma-Aldrich, 47 mm, 0.20 μm pore

size) at 3 L/min for 2 h. The constituents of the filtered aged particles were extracted into 5 mL of 2% methanol–water solution under 30 min sonication for offline measurements. A double beam UV–vis spectrophotometer (UV-6100S, Mapada Instruments) was used to measure the absorbance of the extracts from 200 to 600 nm. The spectrophotometer was blanked using a 1-cm quartz curvette filled with 2% methanol–water solution. Since the extracts were in the form of solutions, they could not be measured by a conventional infrared spectrometer equipped with a KBr beamsplitter. The infrared spectra of the extracts were recorded on an ATR-FTIR (Thermo Nicolet iS 10, Thermo Fisher Scientific) spectrometer equipped with a DTGS detector, which could be used for the determination of solution samples directly. ATR-FTIR was performed in the auto-gain mode, and data were obtained between 4000 and 400 cm^{-1} with a resolution of 2 cm^{-1}.

ALTOFMS measurements of aged *p*-xylene SOA

The aged *p*-xylene SOA particles were measured by ALTOFMS coupled with the FCM clustering algorithm in real time. The aged SOA particles were transferred into the ALTOFMS instrument via an aerodynamic lens and allowed into the sizing system for velocity/size determination and chemical component analysis system sequentially. The particles with measured diameters were ionized by a 248-nm pulsed excimer KrF laser. Although an ultraviolet laser pulse is often used to ionize material from the particle, the laser desorption ionization (LDI) mechanism is not fully understood. It is generally believed that, upon absorption of the laser pulses, the particle is heated rapidly, desorbing and ionizing individual molecules from the particle. As proposed by Reinard and Johnston,[24] ion formation occurs by a two-stage process. In the first stage, photoionization of laser-desorbed neutrals gives rise to cations and free electrons. In the second stage, collisions in the plume cause electron capture and competitive charge transfer. It has been demonstrated that ALTOFMS can be successfully applied to measure organic aerosol particles.[25] Silva and Prather[26] have used ALTOFMS with a Nd:YAG laser operating at 266 nm to analyze organic compounds containing a variety of functional groups, including polycyclic aromatic hydrocarbons, heterocyclic analogs, aromatic oxygenated compounds, aliphatic dicarboxylic acids, and reduced nitrogen species. They found that the positive ion mass spectra of organic compounds are similar to those found in libraries of 70-eV electron impact mass spectrometry in many cases, indicating that most organic compounds can be desorbed and ionized by the ultraviolet laser pulse. As the photon energy of the 248-nm pulsed excimer KrF laser used in this study is greater than that of the Nd:YAG laser used by Silva and Prather, we were confident that most organic components of the aged *p*-xylene SOA could be ionized. The formed ions were analyzed in a linear time-of-flight mass spectrometer. The acquired mass spectra of particles were calibrated with well-known ions for the recorded mass spectra and converted into a normalized 300-point vector. The data vectors of all the particles measured were written into a classification matrix. Each spectrum's data was stored as one row in this matrix. Then, the mass spectra of individual particles were further handled by the FCM algorithm, as described in detail in our previous studies.[17,18]

RESULTS AND DISCUSSION

Effect of NH_3 on the particulate products of aged *p*-xylene SOA without NO

The influence of NH_3 on the particulate products of aged *p*-xylene SOA in the absence of NO was studied first to obtain a reference for comparison. Figure 1 shows the UV–vis spectra of the extracts of aged *p*-xylene SOA in the absence and in presence of 20 ppm NH_3 without NO. These spectra, which have a strong absorption band at 216 nm and a weak absorption peak at 274 nm, are similar to the UV–vis spectra of the phenol solution obtained by Seftel *et al.*[27] As proposed by Seftel *et al.*,[27] the absorption band at 210–220 nm corresponds to the E_2 band of the benzene ring, which is due to the $\pi \rightarrow \pi^*$ transition of three ethylene cyclic conjugated systems, and the absorption band at 270 nm, which is due to the overlap of the $\pi \rightarrow \pi^*$ transition and the vibration of the phenol, is the characteristic absorption peak of phenol. Compared to the absorption band at 270 nm of the phenol solution, the absorption peak at 274 nm of the extract of aged *p*-xylene SOA without NO and NH_3 is red-shifted slightly by about 4 nm.

According to the reaction mechanism proposed by Atkinson *et al.*,[28] OH-initiated reaction with *p*-xylene results in a minor hydrogen abstraction to form the methylbenzyl radical and a major OH addition to the

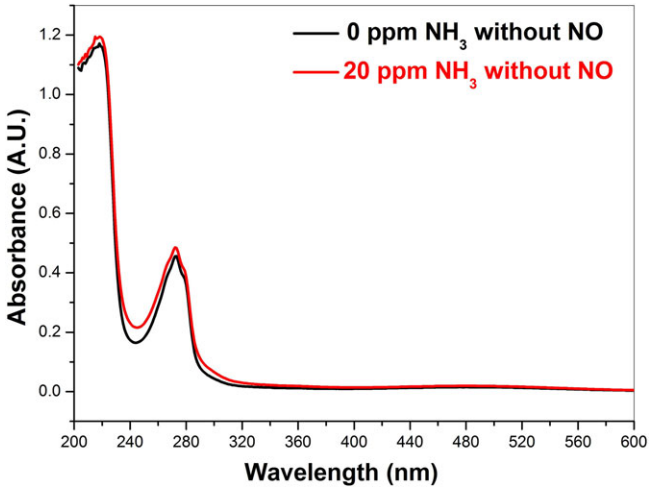

Fig. 1. UV–vis spectra of extract of aged p-xylene SOA in the presence of 0 and 20 ppm NH_3 without NO.

benzene ring to generate the dimethyl hydroxycyclohexadienyl radical. Under atmospheric conditions, the subsequent reactions of these two radicals with O_2 and NO lead to the formation of the 2,5-dimethylphenol, *p*-tolualdehyde, glyoxal, methylglyoxal, and other carbonyl products, as shown in Figure 2. As can be seen from the Figure 2, NO plays a decisive role in the conversion of the peroxy radicals to alkoxy radicals, which can further crack or react with O_2 to produce aldehyde products. Thus, in the photoxidation of *p*-xylene without NO, the reaction channels leading to the formation of carbonyl products are hindered, and the dimethyl hydroxycyclohexadienyl radical reacting with O_2 is the predominant path, indicating that 2,5-dimethylphenol is the major product of aged *p*-xylene SOA in the absence of NO and NH_3. It is obvious that the hydrogen of the benzene ring is substituted by the methyl group, causing the red shift of the absorption peak of 274 nm, as displayed in Figure 1. The phenolic product was further confirmed by the mass spectrum of aged *p*-xylene SOA particles without NO and NH_3 obtained by ALTOFMS. The average mass spectrum of 100 raw spectra of aerosol particles shown in Figure 3 is dominated by the characteristic cleavage fragments of phenolic compounds at *m/z* 93 ($C_6H_5O^+$) and of the benzene ion and its fragment ion peaks at *m/z* 77 ($C_6H_5^+$), 65 ($C_5H_5^+$), 52 (C_4H_4+), 39 ($C_3H_3^+$), and 28 ($C_2H_4^+$).

It is worth noting that the UV–vis spectrum of the extract of aged *p*-xylene SOA in the presence of 20 ppm NH_3 is similar to that of 0 ppm NH_3. Also, the absorbance at 274 nm (corresponding to the content of 2,5-dimethylphenol in aged *p*-xylene SOA) of the extract of aged *p*-xylene SOA in the absence of NO at different concentrations of NH_3 displayed in Figure 4 is nearly identical, suggesting that 2,5-dimethylphenol is the predominant aging product in each case, and NH_3 does not alter the molecular component of aged *p*-xylene SOA in the absence of NO. This is probably due to the fact that NH_3 cannot interact with 2,5-dimethylphenol formed from *p*-xylene reaction with OH radicals and O_2. Thus, NH_3 does not alter the gas–particle partitioning in the photoxidation of *p*-xylene without NO and cannot affect the chemical constituents of aged *p*-xylene SOA without NO.

Size distribution of NH_3-aged *p*-xylene SOA particles with NO

The diameter and constitution of a single aged *p*-xylene SOA particle could be measured simultaneously using ALTOFMS. Because of the large variation of the individual aerosol diameters, the size distribution was determined statistically. As displayed in Figure 5, the aged *p*-xylene SOA particles in the presence of 20 ppm NH_3 with NO are predominant in the form of fine particles, with most of these aged particles being of ~600–1200 nm. It has been shown that these fine particles easily deposit in the alveoli and seriously affect human health.[29] The constituents of NH_3-aged *p*-xylene SOA with NO are discussed in the following sections.

UV–vis and IR spectra of NH_3-aged *p*-xylene SOA with NO

Figure 6 displays the typical UV–vis spectra of the extracts of aged *p*-xylene SOA in the presence of 0 and 20 ppm NH_3 with NO, respectively. From the UV–vis spectra in the range 200–600 nm, it can be observed that NH_3-aged *p*-xylene SOA particles with NO absorb light at wavelengths <300 nm but have negligible absorption in the visible range (300–600 nm). Our results are consistent with those of Li *et al.*,[30] who have studied the optical properties of SOA particles from the photoxidation of aromatic compounds and have found that aromatic SOA particles have no obvious absorption in the visible range. However, the UV–vis spectrum of aged *p*-xylene SOA in the presence of NO but without NH_3 has a distinct absorption signal at 205 nm.

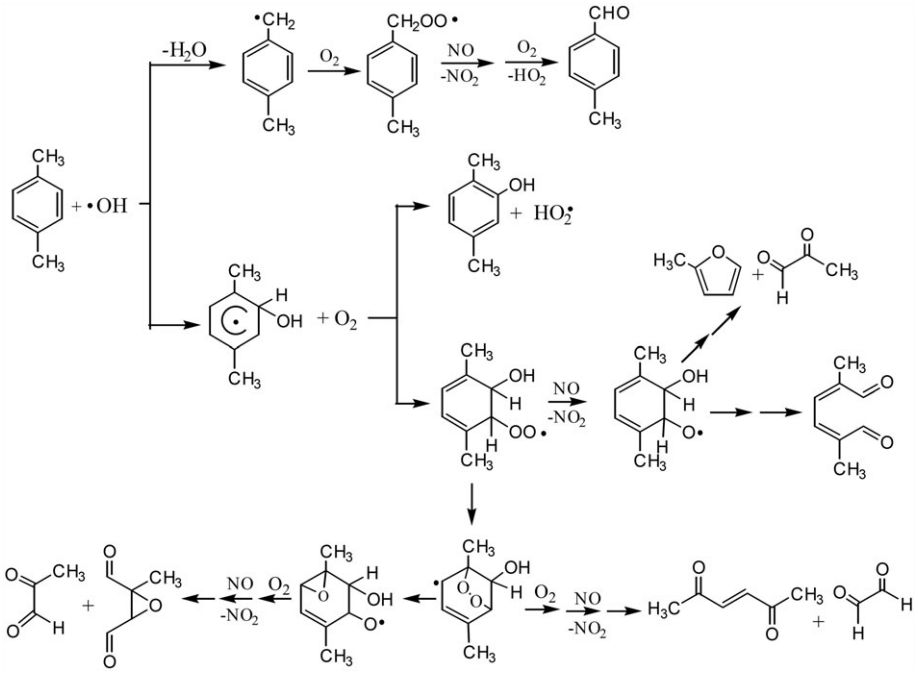

Fig. 2. Proposed reaction mechanism for the OH-initiated oxidation of *p*-xylene.

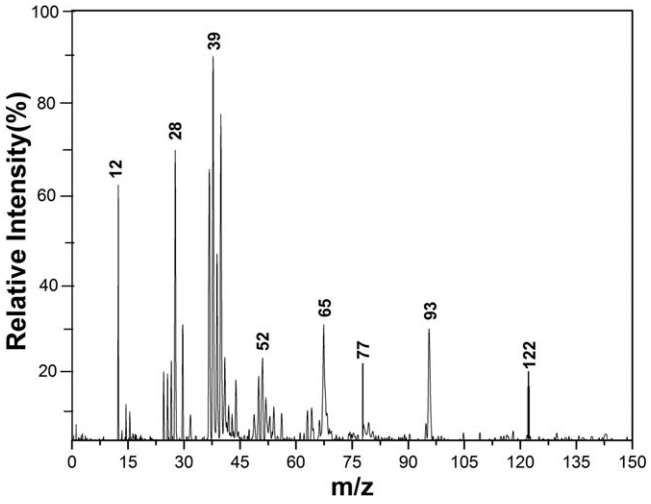

Fig. 3. Average mass spectrum of 100 raw spectra of aged *p*-xylene SOA without NO and NH_3.

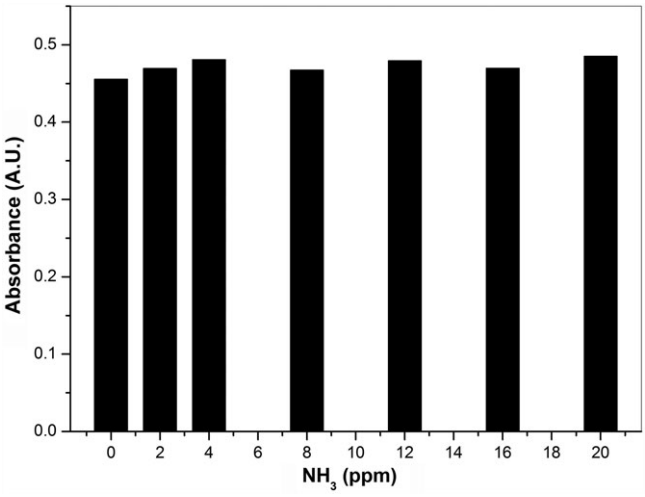

Fig. 4. Absorbance at 274 nm of the filter extract of aged *p*-xylene SOA at different concentrations of NH_3 without NO.

This spectral characteristic matches the light absorption property of a carboxyl compound,[31] indicating that carboxyl compounds are the major constituents of aged *p*-xylene SOA particles in the presence of NO without NH_3. In fact, carboxylic acids such as oxalic acid, *p*-toluic acid, and 2-methyl-4-hydroxy-5-oxo-2-hexaenoic acid have already been shown to be major products in aged *p*-xylene SOA with NO.[16] Also, carboxylic acids were further confirmed by the infrared spectra of the filter extract of aged *p*-xylene SOA in the presence of NO without NH_3, as illustrated in Figure 7. The broad peaks near 3255 and 1643 cm^{-1} were assigned to O—H and unconjugated C=O stretching of carboxyl groups, respectively. The peak at 1055 cm^{-1} could be attributed to the O—H bending vibrations and C—O stretching of carboxyl groups.[32] These peaks lead to the conclusion

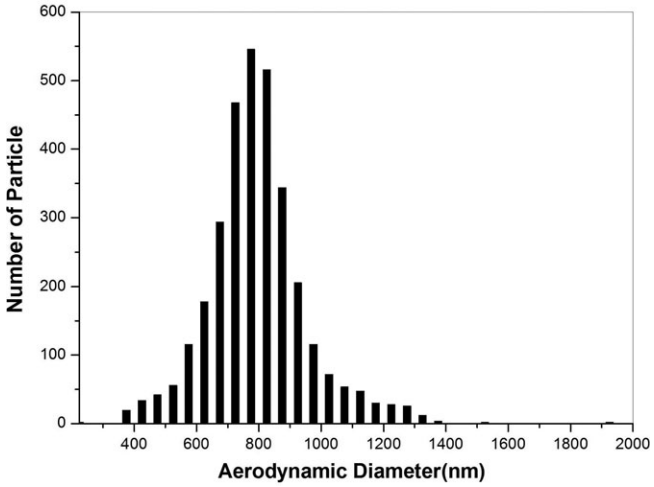

Fig. 5. Size distribution of aged *p*-xylene SOA particles in the presence of 20 ppm NH_3 and 2.0 ppm NO detected by ALTOFMS.

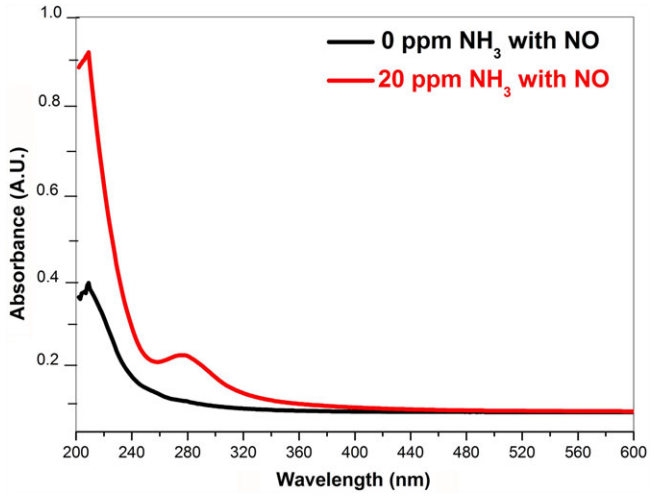

Fig. 6. UV–vis spectra of extract of aged *p*-xylene SOA in the presence of 0 and 20 ppm NH_3 with NO.

that the major products of aged *p*-xylene SOA particles in the presence of NO without NH_3 are carboxylic acids.

Besides the absorption band at 205 nm, there is an additional absorption signal at 280 nm in the UV–vis spectra of extract of aged *p*-xylene SOA with 20 ppm NH_3 and 2.0 ppm NO. It can be seen from Figure 6 that the intensity of the 205 nm absorption peak in the UV–vis spectrum of the extract of aged *p*-xylene SOA in the presence of NO with 20 ppm NH_3 is stronger than that of 0 ppm NH_3, indicating that the content of carboxyl compounds of aged *p*-xylene SOA with NH_3 is higher than that of aged SOA without NH_3. This result provides further evidence that NH_3 can react with gaseous organic acids, generating carboxylates as suggested by Na *et al.*[33] The emergence of the absorption peak at 280 nm indicates the formation of new products in aged *p*-xylene SOA with NH_3 and NO. This band was also observed in evaporating droplets containing glyoxal and $(NH_4)_2SO_4$ conducted by Lee *et al.*[34] and in previous bulk studies[35,36] using solute concentrations of glyoxal and $(NH_4)_2SO_4$ at the molar level. The potential chromophores were likely imidazole compounds, such as imidazole and imidazole-2-carbaldehyde, which were formed from the reactions between NH_3 and carbonyl-containing SOA. Although carboxyl compounds, whose IR absorbance bands shown in Figure 8 (for the aged *p*-xylene SOA with 20 ppm NH_3 and 2.0 ppm NO) appear at 1649 cm^{-1} for the stretching of C═O, 1087 cm^{-1} for the bending vibration of O─H, and stretching of C─O were observed, the notable peaks appear at 1518 cm^{-1} for bending of N─H, 1743–1698 cm^{-1} for stretching of N═C, and 1457 cm^{-1} for stretching of C─N,[8] confirming that the 280 nm chromophores correspond to imidazole compounds. Also, the observed ALTOFMS fragments of CH_2N^+ (*m/z* 28), $C_2H_3N^+$ (*m/z* 41), and $C_3H_3N_2^+$ (*m/z* 67) in the next section indicate that imidazole compounds were formed in the aged *p*-xylene SOA with NH_3 and NO.

Mass spectra of NH_3-aged *p*-xylene SOA with NO

The particulate products of aged *p*-xylene SOA with NO in the absence of NH_3 were already measured by ALTOFMS in our previous study.[16] In addition to the oligomeric components, the mass spectra of aged *p*-xylene SOA in the presence of NO without NH_3 contained the fragment peaks of *m/z* 30 (NO^+), 43 (CH_3CO^+), 44 (CO_2^+), and 46 (NO_2^+), indicating that carbonyl compounds (glyoxal, methylglyoxal, 3-hexene-2,5-dione, 2-furaldehyde, *p*-tolualdehyde, 3-methyl-6-oxo-2,4-heptadieneal, 2-methyl-5-hydroxy-4,6-dioxo-2-hepteneal), caroboxylic acid (oxalic acid, *p*-toluic acid, 2-methyl-4-hydroxy-5-oxo-2-hexaenoic acid), and nitrogen-containing organic compounds (2-nitro-*p*-xylene, *p*-methylbenzyl nitrate) are major products in aged *p*-xylene SOA in the presence of NO without NH_3.[16]

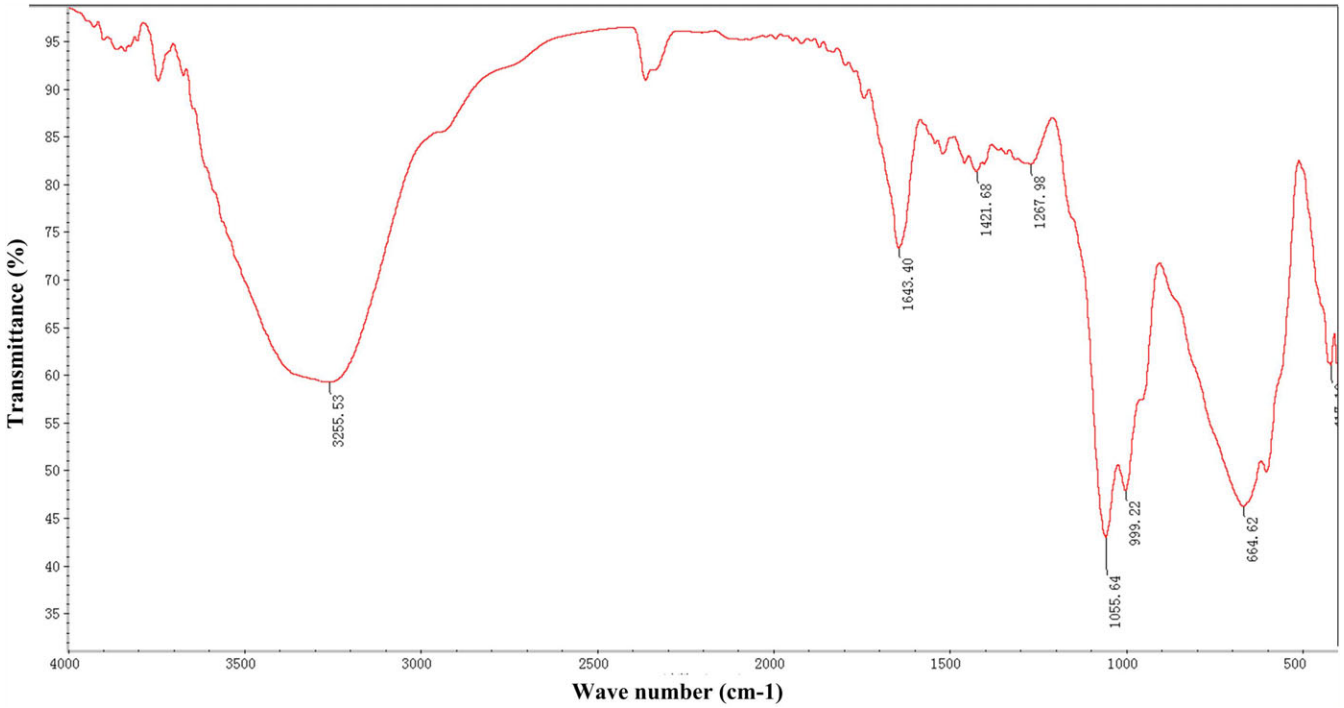

Fig. 7. Infrared spectra of the filter extract of aged *p*-xylene SOA in the presence of NO without NH_3.

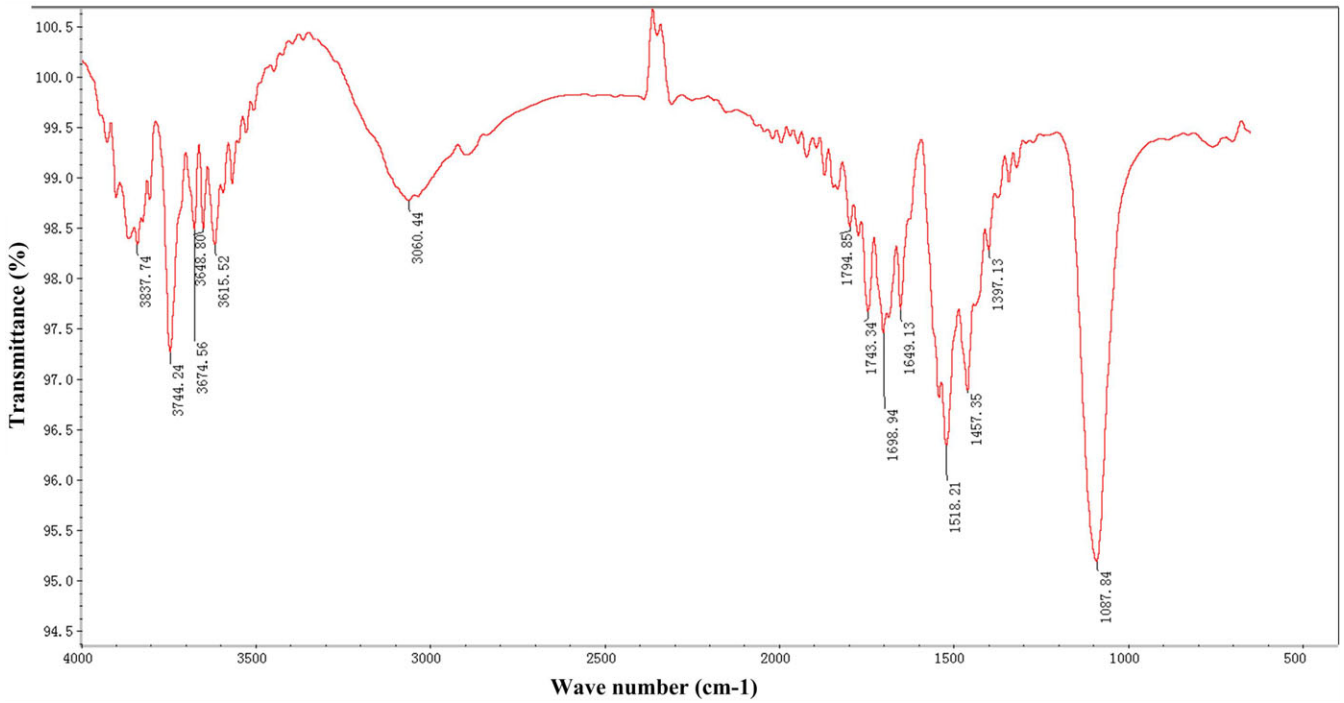

Fig. 8. Infrared spectra of the filter extract of aged *p*-xylene SOA in the presence of 20 ppm NH_3 and 2.0 ppm NO.

About 6500 single-particle mass spectra of aged *p*-xylene SOA in the presence of 20 ppm NH_3 and 2.0 ppm NO were selected to extract potential aerosol with the FCM algorithm. The Davies–Bouldin index shown in Figure 9 has the minimum value at $n = 14$, indicating that the aged *p*-xylene SOA particles in the

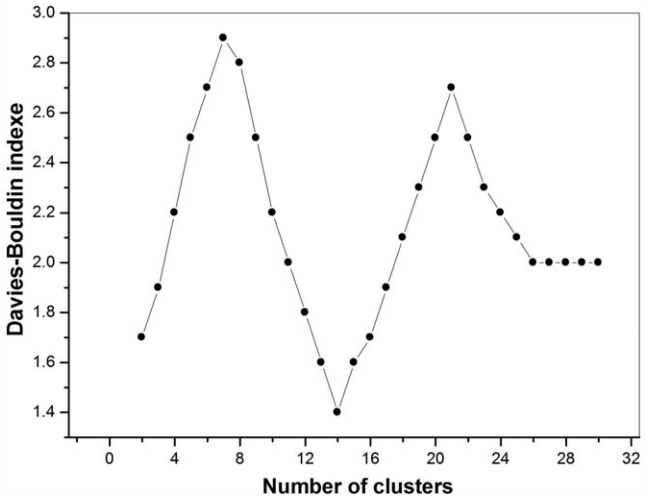

Fig. 9. Clustering number evaluated using the Davies–Bouldin index for aged *p*-xylene SOA particles with 20 ppm NH_3 and 2.0 ppm NO.

presence of 20 ppm NH_3 and 2.0 ppm NO can be clustered into 14 classes. The ion signals of *m*/*z* 18 (NH_4^+) and *m*/*z* 44 (CO_2^+) were found in the mass spectral pattern of Class 1–6 of aged *p*-xylene SOA in the presence of 20 ppm NH_3 and 2.0 ppm NO as shown in Figure 10, demonstrating that organic ammonium carboxylates are the major products in the NH_3-aged *p*-xylene SOA with NO. Glyoxal, methyl glyoxal, *p*-tolualdehyde, 2-methyl-4-hydroxy-5-oxo-2-hexenal, and 2-methyl-6-oxo-2,4-heptadieneal are the major gaseous aldehyde products from the OH-initiated photoxidation of *p*-xylene.[16,37,38] As depicted in Figure 11, the OH radical abstracts a hydrogen atom from the carbonyl group of glyoxal, and an oxygen molecule adds to the radical. The formed peroxy radical can react with the HO_2 radical to form ozone and glyoxylic acid[17,39]. The acid–base neutralization reaction between gaseous glyoxylic acid and the added NH_3 form condensable ammonium glyoxylate (Class 1, molecular ion peak at *m*/*z* 91). Also, glyoxylic acid can further react with the OH radical, oxygen molecule, and HO_2 radical to generate oxalic acid, which further reacts with NH_3 to generate ammonium hydrogen oxalate (Class 3, molecular ion peak at *m*/*z* 107). Similarly, methylglyoxal, *p*-tolualdehyde, 2-methyl-4-hydroxy-5-oxo-2-hexenal, and 2-methyl-6-oxo-2,4-heptadieneal can be oxidized by OH radical, oxygen molecule, and the HO_2 radical to yield methyl glyoxylic acid, *p*-methyl benzoic acid, 2-methyl-4-hydroxy-5-oxo-2-hexaenoic acid, and 2-methyl-5-hydroxy-4,6-dioxo-2-heptennoic acid, respectively. These carboxylic acids can interact with NH_3, producing condensable ammonium methyl glyoxylate (Class 2, molecular ion peak at *m*/*z* 105), *p*-methyl ammonium benzoate (Class 4, molecular ion peak at *m*/*z* 153), ammonium 2-methyl-4-hydroxy-5-oxo-2-hexaenoiclate (Class 5, molecular ion peak at *m*/*z* 175), and ammonium 2-methyl-5-hydroxy-4,6-dioxo-2-heptennoiclate (Class 6, molecular ion peak at *m*/*z* 203), respectively.

As displayed in Figure 10, N-containing fragments appear in the mass pattern of Class 8–14 of aged *p*-xylene SOA in the presence of 20 ppm NH_3 and 2.0 ppm NO. Strong peaks belonging to the $C_xH_yN_n$ dominate the spectrum at m/*z* 28 (CH_2N^+), 41 ($C_2H_3N^+$), and 67 ($C_3H_3N_2^+$), demonstrating that imidazole species are formed in the NH_3-aged *p*-xylene SOA with NO.[17,18] These results are in accordance with those of previous studies, which found a notable increase in the fraction of organonitrogen compounds for aged α-pinene SOA[7] and *m*-xylene SOA with NH_3.[8] It is well known that α-dicarbonyls such as glyxoxal and methylglyxoxal are the major particulate products from the photoxidation of *p*-xylene.[16,37,38] According to the experimental results of Liu *et al.*[8] and Zhang *et al.*,[40] heterogeneous reactions of NH_3 with carbonyl compounds in SOA lead to the generation of imidazole products after the NH_3 uptake onto the SOA. As shown in Figure 12, α-dicarbonyls are protonated by hydrogen ions from organic acid products and hydrolyzed by the diol product (**1**) and the tetrol product (**2**) formation subsequently. Also, the protonated α-dicarbonyls can be attacked by NH_3 followed by the loss of H_2O and H^+ ion, producing the diimine product (**3**). The diimine (**3**) reacts with the tetrol product (**2**) to produce (**4**) via the dehydration reaction of hydrogen atom of amido of (**3**) and the OH of (**2**). Compound (**4**) is unstable, the lone pair electrons of N atom could nucleophilically attack the C atom, leading to the formation of (**5**) after dehydration. Compound (**5**) produces formic acid (or acetic acid) and 1*H*-imidazole (Class 7, molecular ion peak at *m*/*z* 67) or 4-methyl-1*H*-imidazole (Class 8, molecular ion peak at *m*/*z* 82)) through electronic rearrangement and the fracture dehydration reaction. In addition, (**5**) can also undergo electron rearrangement, as shown in Figure 12, to form (**6**), which can be dehydrated to generate imidazole-2-

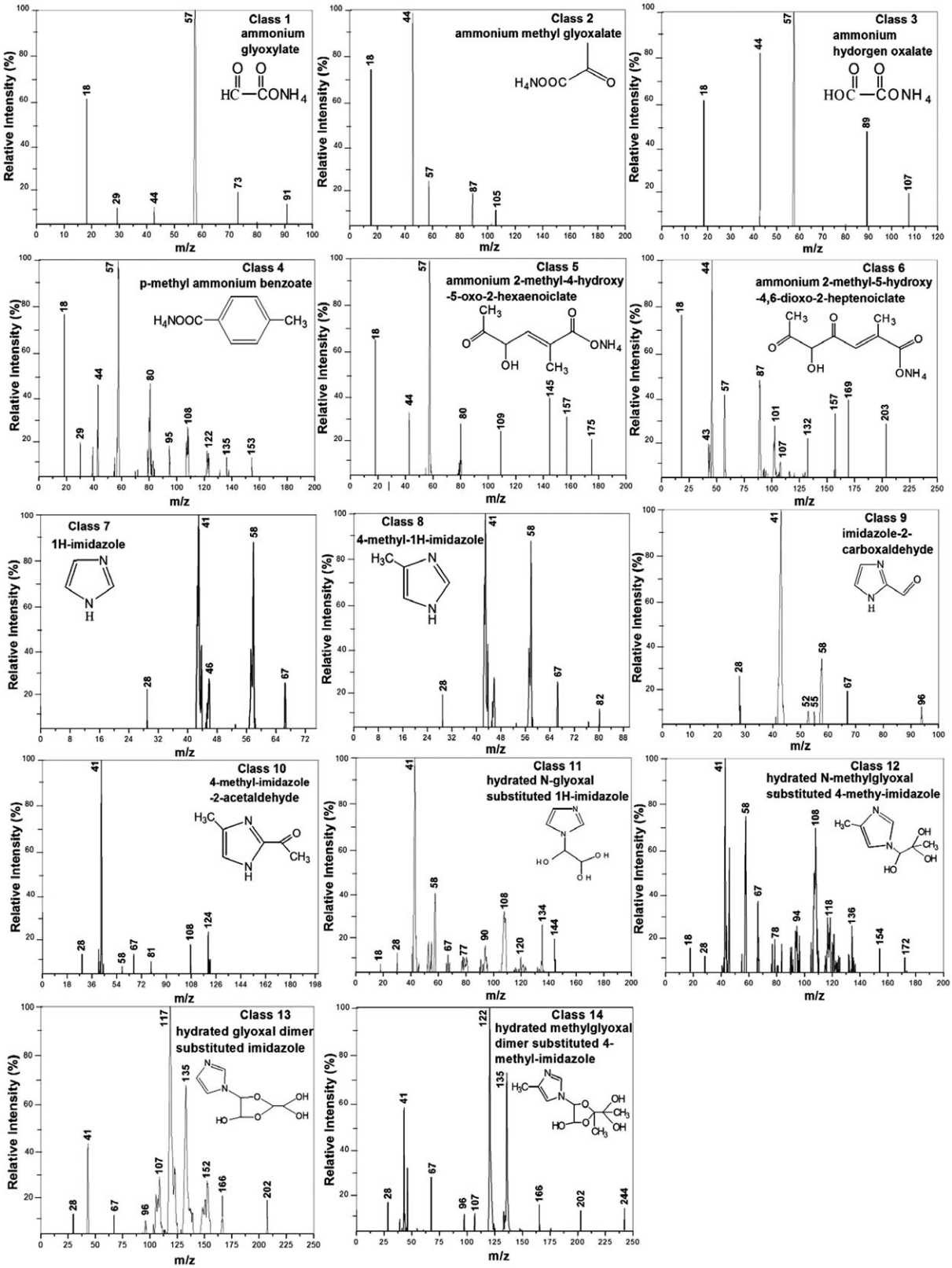

Fig. 10. Representative spectral patterns of aged *p*-xylene SOA particles in the presence of 20 ppm NH_3 and 2.0 ppm NO as determined by FCM.

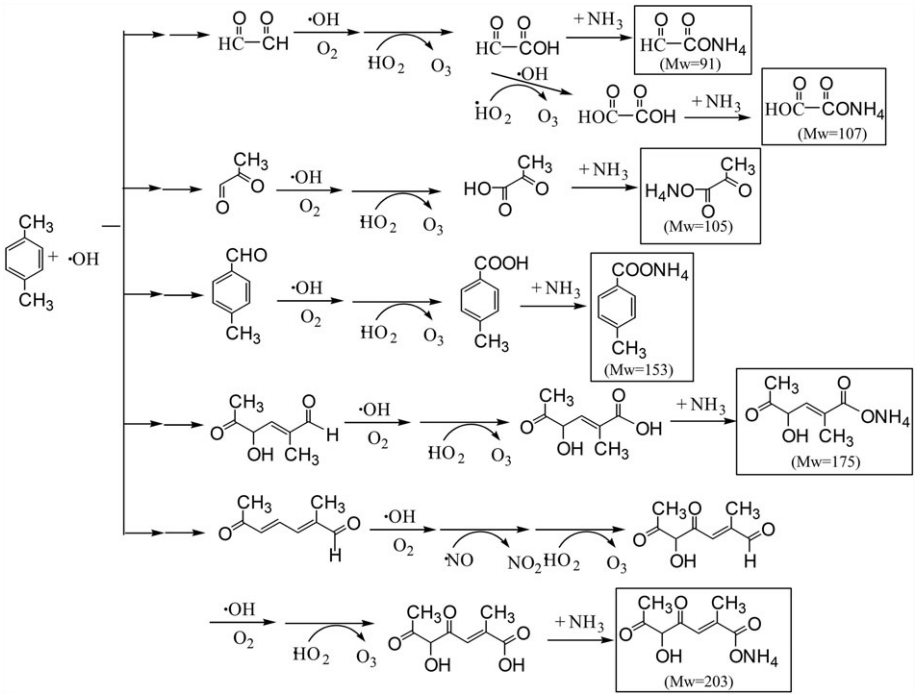

Fig. 11. Proposed aging mechanism leading to the formation of ammonium carboxylates.

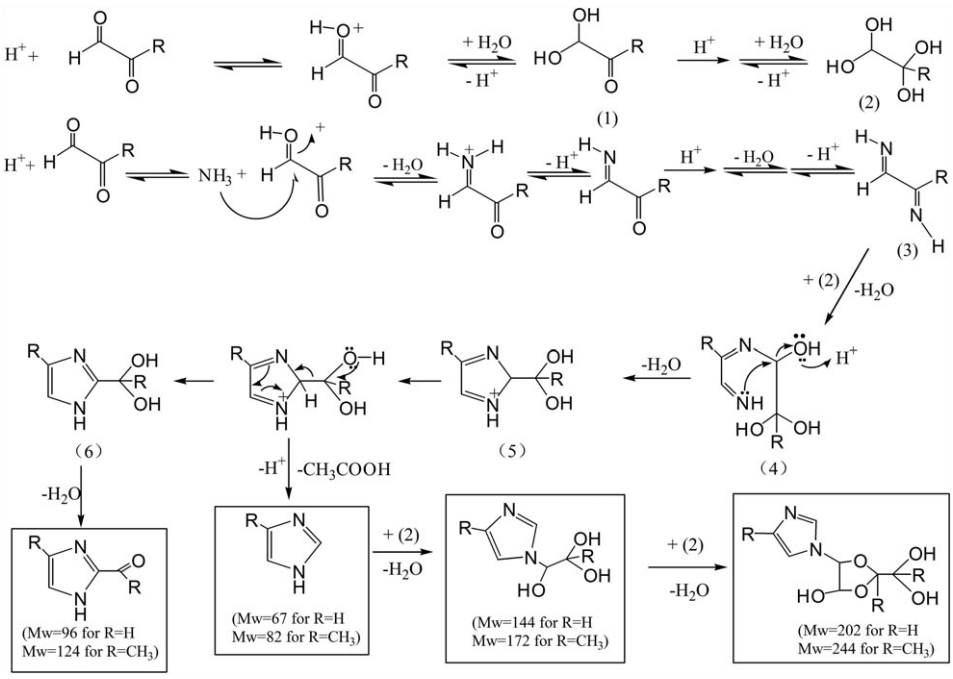

Fig. 12. Proposed aging mechanism leading to the formation of imidazole products (R═H for glyoxal and R═CH_3 for methylglyoxal).

carbaldehyde (Class 9, molecular ion peak at *m*/*z* 96) or 4-methyl-imidazole-2-acetaldehyde (Class 10, molecular ion peak at *m*/*z* 124). The formed 1*H*-imidazole (or 4-methyl-1*H*-imidazole) can continue to react with (**2**) to generate hydrated *N*-glyoxal-substituted 1*H*-imidazole (Class 11, molecular ion peak at *m*/*z* 144) (or hydrated

N-methylglyoxal-substituted 4-methyl-imidazole (Class 12, molecular ion peak at *m*/*z* 172)), and hydrated glyoxal dimer-substituted imidazole (Class 13, molecular ion peak at *m*/*z* 202) (or hydrated methylglyoxal dimer substituted 4-methyl-imidazole (Class 14, molecular ion peak at *m*/*z* 244)) after dehydration, respectively,[32–34] as depicted in Figure 12.

Effect of NH_3 on the particulate products of aged *p*-xylene SOA with NO

To investigate how NH_3 affects the ammonium carboxylates and imidazole products, the UV–vis spectra of filter extracts of aged *p*-xylene SOA with NO at different concentration of NH_3 were measured. As shown in Figure 13, the absorbance at 205 nm (corresponding to the content of ammonium carboxylates in aged *p*-xylene SOA) increases as the added NH_3 increases from 0 to 20 ppm. However, the absorbance of 205 nm remained almost constant as the concentration of NH_3 exceeded 8 ppm, while the absorption peak at 280 nm became discernable and its absorbance increased gradually and reached a plateau after the concentration exceeded 16 ppm. Na *et al.*[33] and Paciga *et al.*[41] studied the neutralization reaction between NH_3 and gaseous organic acids, leading to the generation of particle-phase organic ammonium salts. As reactions of NH_3 with carbonyls are usually acid-catalyzed,[40] Liu *et al.*[8] suggested that the rates of gas-phase reactions between NH_3 and carbonyls are exceedingly slow as a termolecular reaction would be necessary and heterogeneous reactions occur after NH_3 absorbed onto SOA contributes to particulate imidazole products.

Based on the experimental results above, the effects of NH_3 on the ammonium carboxylates and imidazole products can be interpreted. In the gas-phase reaction of organic acids and carbonyls from the photooxidation of *p*-xylene exposed to gaseous NH_3, acid–base neutralization reaction between gas-phase organic acids and NH_3 occurs first. The resulting organic ammonium salts subsequently condense, leading to an increase of organic ammonium in aged *p*-xylene SOA. When the concentration of NH_3 increases to a certain value (8 ppm in this study), the gas-phase organic acids are consumed completely, and the concentration of ammonium carboxylates (corresponding to the absorbance of 205 nm) remains nearly constant even though the concentration of NH_3 increases. Heterogeneous reactions occur via the uptake of NH_3 by *p*-xylene SOA when the concentration of NH_3 exceeds 8 ppm, facilitating the formation of imidazole products as mentioned above. It is not surprising that the concentration of imidazole products (corresponding to the absorbance of 280 nm) increases as the amount of the added NH_3 increases from 8 to 20 ppm. It is worth noting that the generation of no additional imidazole products is observed as the added NH_3 exceeds 16 ppm. This is probably due to the fact that the particulate carbonyls present in this reaction, in terms of NH_3, are consumed totally.

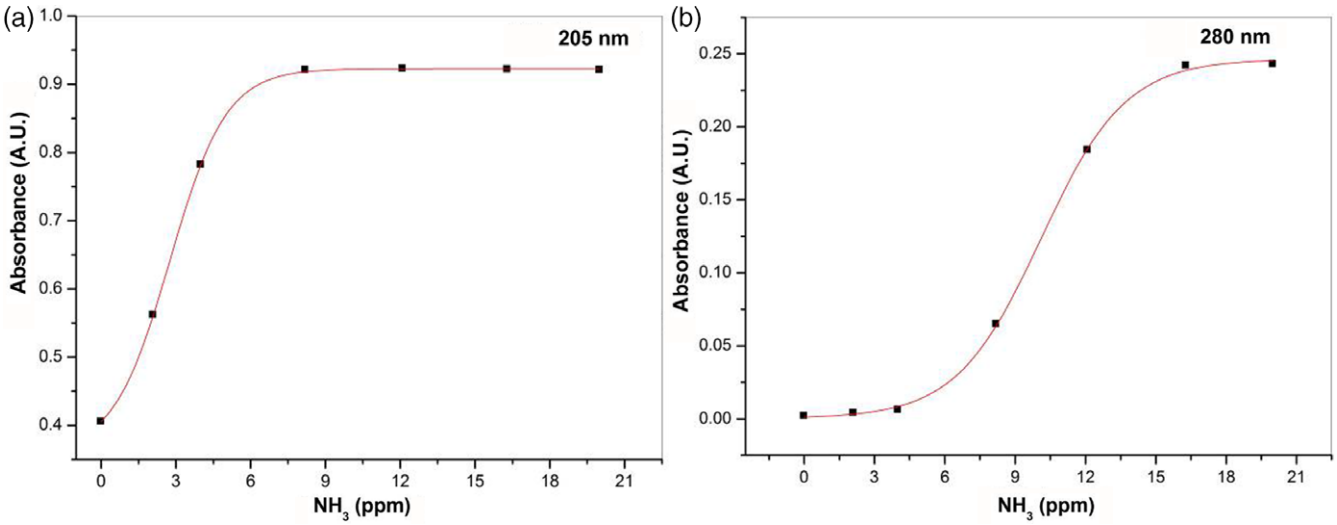

Fig. 13. Absorbance at (a) 205 nm and (b) 280 nm of the filter extract of aged *p*-xylene SOA with NO at different concentration of NH_3.

Compared to the experiments of Na *et al.*[33] and Liu *et al.*,[8] this work has extended the concentration of NH_3 to 20 ppm, and the particulate products of NH_3-aged *p*-xylene SOA with NO measured by ALTOFMS, UV–vis, and ATR-FTIR, further strengthening the suggestion that NH_3 can react with gaseous organic acids generating condensable organic ammonium salts. Also, 1*H*-imidazole, 4-methyl-1*H*-imidazole, and their derivatives, which were formed from the heterogeneous reactions between NH_3 and dialdehydes of SOA, were newly detected. The results of this study also indicated that imidazole derivatives could be formed via the absorption of NH_3 by fresh SOA particles, in contrast to the experimental results of Bones *et al.*[42] where organonitrogen products were found to form over several days. These would provide valuable information on anthropogenic SOA aging and new pathway for NH_3 deposition.

CONCLUSIONS

Smog chamber experiments were performed to investigate the chemical composition and reaction mechanisms for NH_3-aged *p*-xylene SOA in the absence and presence of NO. The chemical constituents of aged p-xylene SOA were measured by UV–vis, ATR-FTIR, and ALTOFMS, which showed that NH_3 does not alter the molecular component of aged *p*-xylene SOA in the absence of NO. Nevertheless, NH_3 can react with gaseous organic acids, generating condensable organic ammonium salts and enhancing SOA formation in the presence of NO. 1*H*-Imidazole, 4-methyl-1*H*-imidazole, and their derivatives formed from heterogeneous reactions between NH_3 and dialdehydes of *p*-xylene SOA with NO were newly detected in this study. Imidazole compounds from this mechanism may be a potential source of ambient particle-associated nitrogen-containing organic compounds. Also, imidazole compounds have been regarded as an important kind of brown carbon, which are considered to have a significant role in climate radiative forcing.[9] The absorption properties of aged aromatic SOA need to be investigated.

ACKNOWLEDGMENTS

The authors thank Mr. Michael Nusbaum, Department of English, Xiamen University, Tan Kah Kee College, for help with the English language. This work was supported by the National Natural Science Foundation of China (No. 41575118, 41305109, 21502086, 41575126), the Outstanding Youth Science Foundation of Fujian Province of China (No. 2015J06009), and the Natural Science Foundation of Fujian Province of China (No. 2015J05028). Also, the authors express their gratitude to the referees for their valuable comments.

REFERENCES

1. P. J. Ziemann, R. Atkinson, *Chem. Soc. Rev.* **2012**, *41*, 6582.
2. L. J. Li, P. Tang, S. S. Nakao, M. Kacarab, D. R. Cocker III, *Environ. Sci. Technol.* **2016**, *50*, 6249.
3. D. R. Gentner, S. H. Jathar, T. D. Gordon, R. Bahreini, D. A. Day, I. E. Haddad, P. L. Hayes, S. M. Pieber, S. M. Platt, J. Gouw, A. H. Goldstein, R. A. Harley, J. L. Jimenez, A. S. H. Prévôt, A. L. Robinson, *Environ. Sci. Technol.* **2017**, *51*, 1074.
4. Y. Rudich, N. M. Donahue, T. F. Mentel, *Annu. Rev. Phys. Chem.* **2007**, *58*, 321.
5. M. O. Andreae, *Science* **2009**, *326*, 1493.
6. K. M. Updyke, T. B. Nguyen, S. A. Nizkorodov, *Atmos. Environ.* **2012**, *63*, 22.
7. J. M. Flores, R. A. Washenfelder, G. Adler, H. J. Lee, L. Segev, J. Laskin, A. Laskin, S. A. Nizkorodov, S. S. Brown, Y. Rudich, *Phys. Chem. Chem. Phys.* **2014**, *16*, 10629.
8. Y. Liu, J. Liggio, R. Staebler, S. M. Li, *Atmos. Chem. Phys.* **2015**, *15*, 13569.
9. A. Laskin, J. Laskin, S. A. Nizkorodov, *Chem. Rev.* **2015**, *115*, 4335.
10. M. O. Andreae, V. Ramanathan, *Science* **2013**, *340*, 280.
11. M. J. Tang, J. M. Alexander, D. Kwon, A. D. Estillore, O. Laskina, M. A. Young, P. D. Kleiber, V. H. Grassian, *J. Phys. Chem. A* **2016**, *120*, 4155.
12. F. Paulot, D. J. Jacob, R. W. Pinder, J. O. Bash, K. Travis, D. K. Henze, *J. Geophys. Res. -Atmos.* **2014**, *119*, 4343.
13. K. Sun, L. Tao, D. J. Miller, D. Pan, L. M. Golston, M. A. Zondlo, R. J. Griffin, H. W. Wallace, Y. J. Leong, M. M. Yang, Y. Zhang, D. L. Mauzerall, T. Zhu, *Environ. Sci. Technol.* **2017**, *51*, 2472.
14. S. K. Sharma, M. Kumar, N. C. Gupta, M. Saxena, T. K. Mandal, *Meteorol. Atmos. Phys.* **2014**, *124*, 67.
15. C. Reche, M. Viana, A. Karanasiou, M. Cusack, A. Alastuey, B. Artiñano, M. A. Revuelta, P. López-Mahía, G. Blanco-Heras, S. Rodríguez, A. M. Sánchez de la Campa, R. Fernández-Camacho, Y. González-Castanedo, E. Mantilla, Y. S. Tang, X. Querol, *Chemosphere* **2015**, *119*, 769.

16. M.-Q. Huang, W.-J. Zhang, L.-Q. Hao, Z.-Y. Wang, W.-W. Zhao, X.-J. Gu, L. Fang, *J. Chin. Chem. Soc.* **2008**, *55*, 456.
17. M.-Q. Huang, J.-H. Zhang, S.-Y. Cai, Y.-M. Liao, W.-X. Zhao, C.-J. Hu, X.-J. Gu, L. Fang, W.-J. Zhang, *J. Atmos. Chem.* **2016**, *73*, 329.
18. M.-Q. Huang, L.-Q. Hao, S.-Y. Cai, X.-J. Gu, W.-X. Zhang, C.-J. Hu, Z.-Y. Wang, L. Fang, W.-J. Zhang, *Atmos. Environ.* **2017**, *152*, 490.
19. Z.-L. Yao, B.-B. Wu, Y.-N. Wu, X.-Y. Cao, X. Jiang, *Atmos. Environ.* **2015**, *123*, 1.
20. R. Atkinson, *Atmos. Environ.* **2000**, *34*, 2063.
21. T. E. Lane, N. M. Donahue, S. N. Pandis, *Environ. Sci. Technol.* **2008**, *42*, 6022.
22. M. Xie, K.-G. Zhu, T.-J. Wang, P.-L. Chen, Y. Han, S. Li, B.-L. Zhuang, L. Shu, *Sci. Total Environ.* **2016**, *551–552*, 533.
23. R. Atkinson, W. P. L. Carter, A. M. Winer, *J. Air Pollut. Control Assoc.* **1981**, *31*, 1090.
24. M. S. Reinard, M. V. Johnston, *J. Am. Soc. Mass Spectrom.* **2008**, *19*, 389.
25. K. A. Pratt, K. A. Prather, *Mass Spectrom. Rev.* **2011**, *31*, 1.
26. P. J. Silva, K. A. Prather, *Anal. Chem.* **2000**, *72*, 3553.
27. E. M. Seftel, M. Niarchos, C. Mitropoulos, M. Mertens, E. F. Vansant, P. Cool, *Catal. Today* **2015**, *252*, 120.
28. R. Atkinson, J. Arey, *Chem. Rev.* **2003**, *103*, 4605.
29. A. Rohr, J. McDonald, *Crit. Rev. Toxicol.* **2016**, *46*, 97.
30. K. Li, W.-G. Wang, M.-F. Ge, J.-J. Li, D. Wang, *Sci. Rep.* **2014**, *4*, 1.
31. A. G. Carlton, B. J. Turpin, K. E. Altieri, S. Seitzinger, A. Reff, H. J. Lim, B. Ervens, *Atmos. Environ.* **2007**, *41*, 7588.
32. J. L. Chang, J. E. Thompson, *Atmos. Environ.* **2010**, *44*, 541.
33. K. Na, C. Song, C. Switzer, D. R. Cocker III. , *Environ. Sci. Technol.* **2007**, *41*, 6096.
34. A. K. Y. Lee, R. Zhao, R. Li, J. Liggio, S. M. Li, P. D. Abbatt, *Environ. Sci. Technol.* **2013**, *47*, 12819.
35. C. J. Kampf, R. Jakob, T. Hoffmann, *Atmos. Chem. Phys.* **2012**, *12*, 6323.
36. A. Maxut, B. Nozière, B. Fenet, H. Mechakra, *Phys. Chem. Chem. Phys.* **2015**, *17*, 20416.
37. R. Volkamer, U. Platt, K. Wirtz, *J. Phys. Chem. A* **2001**, *105*, 7865.
38. D. Johnson, M. E. Jenkin, K. Wirtz, M. Martin-Reviejo, *Environ. Chem.* **2005**, *2*, 35.
39. K. Sato, A. Takami, Y. Kato, T. Seta, Y. Fujitani, T. Hikida, A. Shimono, T. Imamura, *Atmos. Chem. Phys.* **2012**, *12*, 4667.
40. R. Zhang, G. Wang, S. Guo, M. L. Zamora, Q. Ying, Y. Lin, W.-G. Wang, M. Hu, Y. Wang, *Chem. Rev.* **2015**, *115*, 3803.
41. A. L. Paciga, I. Riipinen, S. N. Pandis, *Environ. Sci. Technol.* **2014**, *48*, 13769.
42. D. L. Bones, D. K. Henricksen, S. A. Mang, M. Gonsior, A. P. Bateman, T. B. Nguyen, W. J. Cooper, S. A. Nizkorodov, *J. Geophys. Res.-Atmos.* **2010**, *115*, D05203.

